Top-Bottom Interference Effects in Higgs Plus Jet Production at the LHC

Jonas M. Lindert,[1,*] Kirill Melnikov,[2,†] Lorenzo Tancredi,[2,‡] and Christopher Wever[2,3,§]
[1]*Institute for Particle Physics Phenomenology, Durham University, Durham DH1 3LE, United Kingdom*
[2]*Institute for Theoretical Particle Physics (TTP), KIT, 76128 Karlsruhe, Germany*
[3]*Institut für Kernphysik (IKP), KIT, 76344 Eggenstein-Leopoldshafen, Germany*
(Received 18 March 2017; published 22 June 2017)

We compute next-to-leading order QCD corrections to the top-bottom interference contribution to $H + j$ production at the LHC. To achieve this, we combine the recent computation of the two-loop amplitudes for $gg \to Hg$ and $qg \to Hq$, performed in the approximation of a small b-quark mass, and the numerical calculation of the squared one-loop amplitudes for $gg \to Hgg$ and $qg \to Hqg$, performed within OpenLoops. We find that QCD corrections to the interference are large and similar to the QCD corrections to the top-mediated Higgs production cross section. We also observe a significant reduction in the mass-renormalization scheme uncertainty once the next-to-leading order QCD prediction for the interference is employed.

DOI: 10.1103/PhysRevLett.118.252002

Detailed exploration of the Higgs boson properties is a major part of the physics program at the Large Hadron Collider (LHC). It is hoped that studies of the Higgs couplings will reveal possible physics beyond the standard model (BSM), especially if it mostly manifests itself through interactions with the Higgs bosons. The goal, therefore, is to precisely measure Higgs boson couplings to various particles in the standard model and to search for small deviations. For example, assuming that the energy scale of new physics is close to 1 TeV, generic modifications of the Higgs couplings are expected at the level of $v^2/(1\ \mathrm{TeV})^2 \sim 5 \times 10^{-2}$, where we used $v = 246$ GeV for the Higgs field vacuum expectation value. A variety of explicit BSM scenarios conforms with these expectations [1], suggesting that achieving a few percent precision in studies of the Higgs couplings may indeed provide interesting information about physics beyond the standard model.

Compared to these theoretical goals, existing measurements leave much to be desired [2]. Currently, Higgs couplings to electroweak gauge bosons are known to a precision of between ten and twenty percent and those to third generation fermions to about hundred percent. The couplings to first and second generation fermions are practically unconstrained. It is expected that the situation will dramatically improve with the continued operation of the LHC. For example, it is estimated [3] that by the end of the high-luminosity phase, the Higgs couplings will be determined within a few percent precision. There are several unknowns that may affect the validity of these projections, including progress in reducing the uncertainties in theoretical predictions and the ability of experimentalists to come up with new ideas but, barring revolutionary breakthroughs, these estimates give us a ballpark of what can be expected.

Determination of Higgs couplings at the LHC requires precise theoretical predictions for relevant observables. A case in point is the Higgs boson transverse momentum distribution, whose theoretical understanding is important to properly describe the kinematics of the Higgs decay products but may also give us access to physics beyond the standard model [4].

Higgs bosons at the LHC are mostly produced in gluon collisions. If additional gluons are radiated, a Higgs boson recoils against them; this mechanism leads to a nontrivial Higgs $p_\perp$ spectrum, whose theoretical description requires good understanding of QCD dynamics. For a pointlike Higgs-gluon coupling, perturbative QCD (pQCD) provides an established framework to describe the Higgs $p_\perp$ spectrum, including fixed-order QCD computations recently extended to next-to-next-to-leading order (NNLO) [5] and the resummation computations known in the next-to-next-to-leading logarithmic (NNLL) approximation [6,7]. However, the Higgs coupling to gluons in the standard model (SM) arises only at the quantum level through the fluctuation of gluons into quark-antiquark pairs. Because of the differences in fermion Yukawa couplings, the largest contribution to the ggH coupling in the standard model comes from top quark loops, followed by bottom and charm loops. For values of the Higgs transverse momentum $p_\perp \ll m_t$, the top loop contribution can be considered pointlike to a very good approximation, and we can apply the full power of pQCD to describe it with high precision. However, the bottom and charm loops are not pointlike for moderate values of the transverse momentum, and their treatment in perturbative QCD is much less understood.

Moreover, it is known that the bottom and charm quark contributions to $gg \to Hg$ amplitudes develop a peculiar Sudakov-like dependence on the Higgs boson transverse momentum [9,10]. Taking the bottom quark contribution as an example, we find $A^b_{gg\to Hg} \sim m_b^2/m_H^2 \log^2(p_\perp^2/m_b^2)$ [11]. These double logarithms are not accounted for in the standard resummation framework [12,14] and they significantly enhance the contribution of bottom loops to the Higgs production cross section in gluon fusion, compared to naive

expectations. In fact, the bottom loop contribution to Higgs production in the standard model is estimated to be close to minus five percent [15] and therefore, significant on the scale of the $\mathcal{O}(1\%)$ precision goal discussed above.

It is interesting to remark that the "substructure" of the ggH coupling is precisely what makes the Higgs transverse momentum distribution an interesting observable from the point of view of physics beyond the standard model. For example, current constraints on the charm Yukawa coupling are weak but, if the charm Yukawa coupling deviates significantly from its standard model value, the charm contribution to $gg \to H$ increases, and the relevance of the $c\bar{c} \to H$ annihilation channel for Higgs production grows. These modifications may result in observable effects in the Higgs transverse momentum distribution. It was pointed out in Ref. [16] that studies of the Higgs boson transverse momentum distribution lead to very competitive constraints on the charm Yukawa coupling; for example, it is expected [16] that at high-luminosity LHC, the charm Yukawa coupling can be constrained to lie in the interval $y_c/y_c^{\mathrm{SM}} \in [-2.9, 4.2]$ at the 95% confidence level.

This discussion suggests that the shape of the Higgs boson transverse momentum distribution, from moderate to high $p_\perp$ values, is important for a proper description of the kinematic features of Higgs bosons produced at the LHC and also may provide important information about physics beyond the standard model. Accurate standard model predictions for this observable are key for achieving these goals. As we already mentioned, the pQCD description of the Higgs boson transverse momentum distribution, in the approximation of the pointlike ggH coupling, is rather advanced, see Refs. [5,17], but there is very little understanding of how its not-pointlike component is affected by QCD radiative corrections. To clarify this issue, we report on the computation of QCD radiative corrections to top-bottom interference contribution to Higgs boson production at the LHC in this Letter.

The calculation of the NLO QCD corrections to the top-bottom interference is nontrivial. The leading-order production of the Higgs boson with nonvanishing transverse momentum occurs in different partonic channels, namely $gg \to Hg$, $qg \to Hq$, $\bar{q}g \to H\bar{q}$, and $q\bar{q} \to Hg$. At leading order, these processes are mediated by top or bottom loops (the charm contribution in the SM is negligible). The one-loop amplitudes are known exactly as functions of external kinematic variables and the quark masses [9].

At NLO, the production cross section receives contributions from real and virtual corrections. Since the leading-order process only occurs at one loop, the virtual corrections require two-loop computations that include planar and nonplanar box diagrams with internal masses. The computation of such Feynman diagrams is a matter of active current research that includes attempts to develop efficient numerical methods that can be used in physical kinematics [18] and to extend existing analytic methods to make them applicable to two-loop Feynman diagrams with internal masses [19].

However, if we focus on the top-bottom interference and its impact on Higgs production at the LHC, we can simplify the calculation by using the fact that the mass of the b quark $m_b \sim 4.7$ GeV is numerically small. Indeed, since $m_b \ll m_H, p_\perp^{\mathrm{typ}}$, where $p_\perp^{\mathrm{typ}} \sim 30$ GeV is a typical Higgs boson transverse momentum, Feynman diagrams that describe Higgs production can be expanded in series in m_b for the purposes of LHC phenomenology. We have checked at leading order that the use of scattering amplitudes either exact or expanded in m_b leads to, *at most*, a few percent difference in the interference contribution to the Higgs $p_\perp$ distribution, down to $p_\perp \sim 10$ GeV. Since the interference contribution changes the Higgs boson transverse momentum spectrum by $\mathcal{O}(5\%)$ at leading order, the percent difference between expanded and not expanded results is irrelevant for phenomenology.

Unfortunately, the expansion in m_b is nontrivial since the Higgs boson production cross section depends logarithmically on the b-quark mass. Therefore, we need to devise a procedure to expand scattering amplitudes in m_b and extract the nonanalytic terms. This can be done by deriving differential equations for master integrals that are needed to describe the two-loop corrections to $pp \to H + j$ and then solving them in the limit $m_b \to 0$ [20]. Indeed, since we can derive differential equations to describe the dependence of the master integrals on the mass parameter m_b and on the Mandelstam kinematic variables, and since all the information about singular points of a particular Feynman integral is contained in the differential equations that this Feynman integral satisfies, we can systematically solve the differential equation in a series of m_b and extract the nonanalytic behavior. We note that a similar method was used to compute the top-bottom interference contribution to the inclusive Higgs production cross section in Ref. [21].

We have used this method to calculate all the relevant two-loop scattering amplitudes to describe the production of a Higgs boson in association with a jet [20,22]. In our computation, all quarks in the initial and final states are massless, so that b-initiated processes are not included. The two-loop amplitudes mediated by top quark loops, required to describe the interference, are computed in the approximation of an infinitely heavy top quark [23].

To produce physical results for $H + j$ production, we need to combine the virtual corrections discussed above with the real corrections that describe inelastic processes, e.g., $gg \to H + gg$, $qg \to Hq + g$ etc. Computation of one-loop scattering amplitudes for these inelastic processes is nontrivial; it requires the evaluation of five-point Feynman integrals with massive internal particles. Nevertheless, such amplitudes are known analytically since long ago [24] and were recently reevaluated in Ref. [25].

In this Letter, we follow a different approach, based on the automated numerical computation of one-loop scattering

amplitudes developed in recent years. One such approach, known as OpenLoops [26], employs a hybrid tree-loop recursion. Its implementation is publicly available [27] and has been applied to compute one-loop QCD and electroweak corrections to multileg scattering amplitudes for a variety of complicated processes (see, e.g., Refs. [28,29]) and as an input for the real-virtual contributions in NNLO computations (see, e.g., Ref. [30]).

For applications in NNLO calculations, and similarly for the loop-induced process discussed in this Letter, the corresponding one-loop real contributions need to be computed in kinematic regions where one of the external partons becomes soft or collinear to other partons. A reliable computation in such kinematic regions is nontrivial, but OpenLoops appears to be perfectly capable of coping with this challenge thanks to the numerical stability of the employed algorithms. An important element of this stability is the employed tensor integral reduction library collier [31].

We have implemented all virtual and real amplitudes in the powheg-box [32], where infrared singularities are regularized via Frixione-Kunszt-Signer (FKS) subtraction [33]. All OpenLoops amplitudes are accessible via a process-independent interface developed in Ref. [29]. The implementation within the powheg-box will allow for an easy matching of the fixed-order results presented here with parton showers at NLO. At leading order, this has been done in Ref. [34].

Using the methods described above, we calculated the NLO QCD corrections to the top-bottom interference contribution to $H+j$ production in hadron collisions. We identify the interference contribution through its dependence on top-bottom Yukawa couplings. For the Higgs production cross section, we write

$$d\sigma = d\sigma_{tt} + d\sigma_{tb} + d\sigma_{bb}, \tag{1}$$

where individual contributions to the differential cross section scale as $d\sigma_{tt} \sim \mathcal{O}(y_t^2)$, $d\sigma_{tb} \sim \mathcal{O}(y_t y_b)$, $d\sigma_{bb} \sim \mathcal{O}(y_b^2)$. Given the hierarchy of the Yukawa couplings $y_t \sim 1 \gg y_b \sim 10^{-2}$, the last term in Eq. (3) can be safely neglected. Note, however, that if one focuses on Higgs-related observables that are inclusive with respect to the QCD radiation, $d\sigma_{bb}$ receives contributions from Higgs boson production in association with b quarks, e.g., $gg \to Hbb$. These processes change inclusive Higgs boson observables at below a permille level, which makes them irrelevant unless b jets in the final state are tagged.

Our main focus is the top-bottom interference contribution $d\sigma_{tb}$. Considering the virtual corrections, we write

$$d\sigma_{tb}^{\text{virt}} \sim \text{Re}\left[A_t^{\text{LO}} A_b^{\text{LO}*} + \frac{\alpha_s}{2\pi}\left(A_t^{\text{NLO}} A_b^{\text{LO}*} + A_t^{\text{LO}} A_b^{\text{NLO}*}\right)\right]. \tag{2}$$

The leading-order (one-loop) term in this formula is known, including full mass dependence. The NLO (two-loop) amplitudes with the top quark A_t^{NLO} are only known in the limit $m_t \to \infty$. Since as an input for the NLO calculation we only require the finite reminder of the virtual amplitude A_t^{NLO}, we can safely use the corresponding finite reminder of $A_t^{\text{NLO}}(m_t \to \infty)$ as its approximation. In principle, one can improve on this by computing $1/m_t$ corrections to $A_t^{\text{NLO}}(m_t \to \infty)$, see Ref. [35], but it is not expected that they will have significant impact on the interference at moderate values of the Higgs transverse momentum $p_\perp < m_t$. The real emission contributions are computed with exact top- and bottom-mass dependence throughout the Letter.

In what follows, we present the QCD corrections to the top-bottom interference contribution to the Higgs boson transverse momentum distribution and to the Higgs rapidity distribution in $H+j$ production. We consider proton collisions at the 13 TeV LHC and take the mass of the Higgs boson to be $m_H = 125$ GeV.

We work within a fixed flavor-number scheme and do not consider bottom quarks as partons in the proton. We use the NNPDF3.0 set of parton distribution functions (PDFs) [36]. We also use the strong coupling constant $\alpha_s(m_Z)$ that is provided with this PDF set. We renormalize the b-quark mass in the on-shell scheme and use $m_b = 4.75$ GeV as its numerical value. We choose renormalization and factorization scales to be equal and take, as the central value $\mu = H_T/2$, $H_T = \sqrt{m_H^2 + p_\perp^2} + \sum_j p_{\perp,j}$, where the sum runs over all partons in the final state.

To quantify the impact of the top-bottom interference on an observable $\mathcal{O}$, it is convenient to define the following quantity

$$\mathcal{R}_{\text{int}}[\mathcal{O}] = \frac{\int d\sigma_{tb}\,\delta(\mathcal{O} - \mathcal{O}(\vec{x}))}{\int d\sigma_{tt}\,\delta(\mathcal{O} - \mathcal{O}(\vec{x}))}, \tag{3}$$

where $\vec{x}$ is a set of phase-space variables. Note that we do not expand the σ_{tt} cross section in the denominator in Eq. (3) in powers of α_s. Therefore, any change in $\mathcal{R}_{\text{int}}$ in consecutive orders in perturbation theory would reflect *differences* in QCD corrections to the tb interference and the pointlike contribution to $H+j$ production. In what follows, we present $\mathcal{R}_{\text{int}}$ as a function of the Higgs boson transverse momentum $p_\perp$ and the (pseudo)rapidity η_H.

The impact of the top-bottom interference on the Higgs boson transverse momentum distribution is shown in Fig. 1. We observe that the leading-order interference changes the Higgs boson transverse momentum distribution by -8% at $p_\perp \sim 20$ GeV and $+2\%$ at $p_\perp \sim 100$ GeV. Since the QCD corrections to color-singlet production in gluon annihilation are large, and since it is not clear *a priori* if the QCD corrections to the interference are similar to the QCD corrections to the pointlike cross section, large modifications of these LO results cannot be excluded. The NLO computation, illustrated in Fig. 1, clarifies this point. There, filled bands in blue for the leading and red for

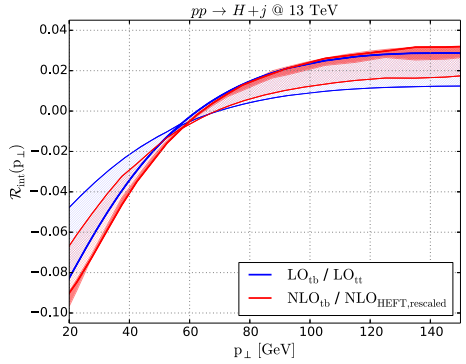

FIG. 1. Relative top-bottom interference contribution to the transverse momentum distribution of the Higgs boson at leading (blue) and next-to-leading (red) order in perturbative QCD. At next-to-leading order, the interference contribution is shown with respect to the pointlike Higgs effective field theory prediction, rescaled with exact leading-order top mass dependence. Filled bands, hardly visible at leading order, show the change in $\mathcal{R}_{\rm int}$, caused by a variation of the renormalization and factorization scales, correlated between the numerator and denominator. The hashed bands indicate the uncertainty due to mass-renormalization scheme variation. See text for details.

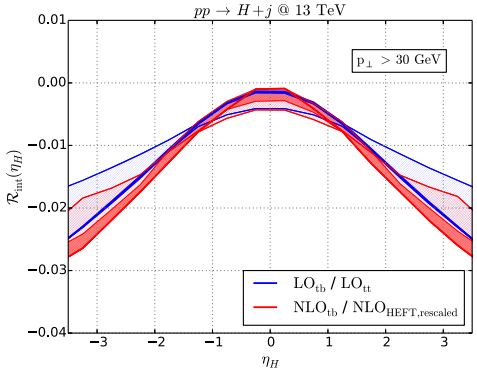

FIG. 2. Relative top-bottom interference contribution to the pseudorapidity distribution of the Higgs boson at leading and next-to-leading order in perturbative QCD. Bands and colors as in Fig. 1.

the next-to-leading order predictions show the result for $\mathcal{R}_{\rm int}(p_\perp)$, computed in the pole mass renormalization scheme. The widths of the bands indicate changes in the predictions caused by variations of renormalization and factorization scales by a factor of two around the central value $\mu = H_T/2$. In fact, we observe that differences between leading and next-to-leading order are very small. For example, $\mathcal{R}_{\rm int}^{\rm NLO}(p_\perp)$ appears to be smaller than $\mathcal{R}_{\rm int}^{\rm LO}(p_\perp)$ by less than a percent at $p_\perp < 60$ GeV and practically coincides with it at higher values of $p_\perp$. We emphasize that these small changes in $\mathcal{R}_{\rm int}$ imply *sizable* $\mathcal{O}(40$–$50\%)$ corrections to the tb interference proper that, however, appear to be very similar to NLO QCD corrections to the pointlike cross section σ_{tt}. The scale variation bands are very narrow (at leading order, hardly visible) due to a cancellation of large scale variation changes between the numerator and denominator in Eq. (3). Similar results for the Higgs boson rapidity distribution for events, with $p_\perp > 30$ GeV, are shown in Fig. 2.

The above result for the scale variation suggests that the uncertainties in predicting the size of top-bottom interference effects in $H + j$ production are small since both the size of corrections and the scale variation bands are similar to the corrections to the pointlike $pp \to H + j$ cross section. Such a conclusion, nevertheless, misses an important source of uncertainties related to a possible choice of a different mass-renormalization scheme. Indeed, since the leading-order interference contribution is proportional to the square of the bottom mass $R_{\rm int} \sim m_b^2$, and since at leading order a change in the mass renormalization scheme simply amounts to the use of different numerical values for m_b in calculating $\mathcal{R}_{\rm int}$, it is easy to see that this ambiguity is very significant. Indeed, suppose that we choose to renormalize the bottom mass in the $\bar{\rm MS}$ scheme and we take $m_b = m_b^{\bar{\rm MS}}(100\ {\rm GeV}) = 3.07$ GeV as an input parameter [37]. Since $[m_b^{\bar{\rm MS}}(100\ {\rm GeV})/m_b^{\rm pole}]^2 \approx 0.4$, this implies that $\mathcal{R}_{\rm int}^{\rm LO}$ is reduced by more than a factor of two, practically independent of the $p_\perp$ value. This large leading-order variation is shown as a hashed blue band in Figs. 1 and 2, where we have taken $m_b = m_b^{\rm pole}$ and $m_b = m_b^{\bar{\rm MS}}(100\ {\rm GeV})$ as the two boundary values.

This large ambiguity in the leading-order value of $\mathcal{R}_{\rm int}$ is somewhat reduced at next-to-leading order, where the effect of the mass renormalization scheme change is less dramatic but, nevertheless, significant. The scheme dependence at NLO for the setup explained in the previous paragraph is shown as a hashed red band. For $p_\perp < 60$ GeV, the mass renormalization scheme uncertainty is reduced by almost a factor of two, whereas the reduction of uncertainty is only marginal at higher $p_\perp$. This happens because at high transverse momenta, there is a significant cancellation between $A_t^{\rm NLO} A_b^{\rm LO*}$ and $A_t^{\rm LO} A_b^{\rm NLO*}$, cf. Eq. (2). Since the first term involves leading order b-quark contributions, it experiences large variations when the b-quark mass renormalization scheme is changed, and this causes large variations in $\mathcal{R}^{\rm int}$ at high $p_\perp$. The interference contribution to the Higgs rapidity distribution in Fig. 2 shows similar features. The mass variation band at NLO is smaller than the LO variation band at large absolute values of the pseudorapidity (small $p_\perp$) and practically indistinguishable from it at the central rapidity values (large $p_\perp$).

In summary, we computed the NLO QCD corrections to the top-bottom interference contribution to Higgs boson production in association with a jet at the LHC. This is the first computation of QCD radiative corrections to Higgs production at this order in perturbation theory that goes beyond the pointlike approximation for the ggH coupling. Our results show that corrections to the

interference are large, yet they appear to track very well corrections to the pointlike component of the cross section. The strong dependence of the LO interference on the mass-renormalization scheme is reduced at NLO, but at high values of the Higgs transverse momentum or at central rapidity, the remaining ambiguities are significant. It is not clear how the situation at high $p_\perp$ and/or small absolute η_H can be further improved. However, we want to emphasize that in these kinematic regions, the interference is numerically small compared to the $\mathcal{O}(y_t^2)$ contribution. Nevertheless, with this result at hand, one can try to provide the best possible theoretical predictions for the Higgs transverse momentum distribution that combine the known results for the $p_\perp$ resummation NNLO corrections to $H + j$ in the pointlike approximation with the top-bottom interference. All the ingredients are now available. We plan to return to this problem before long.

We thank Tomas Jezo for valuable help with the POWHEG-BOX and Fabrizio Caola for useful conversations. The research of K. M. was supported by the German Federal Ministry for Education and Research (BMBF) under Grant No. 05H15VKCCA.

*jonas.m.lindert@durham.ac.uk
†kirill.melnikov@kit.edu
‡lorenzo.tancredi@kit.edu
§christopher.wever@kit.edu

[1] R. S. Gupta, H. Rzehak, and J. D. Wells, Phys. Rev. D **88**, 055024 (2013).
[2] G. Aad *et al.* (ATLAS and CMS Collaborations), J. High Energy Phys. 08 (2016) 045.
[3] (CMS Collaboration), arXiv:1307.7135.
[4] M. Grazzini, A. Ilnicka, M. Spira, and M. Wiesemann, J. High Energy Phys. 03 (2017) 115.
[5] X. Chen, T. Gehrmann, E. W. N. Glover, and M. Jaquier, Phys. Lett. B **740**, 147 (2015); R. Boughezal, F. Caola, K. Melnikov, F. Petriello, and M. Schulze, Phys. Rev. Lett. **115**, 082003 (2015); F. Caola, K. Melnikov, and M. Schulze, Phys. Rev. D **92**, 074032 (2015); X. Chen, J. Cruz-Martinez, T. Gehrmann, E. W. N. Glover, and M. Jaquier, J. High Energy Phys. 10 (2016) 066; R. Boughezal, C. Focke, W. Giele, X. Liu, and F. Petriello, Phys. Lett. B **748**, 5 (2015).
[6] G. Bozzi, S. Catani, D. de Florian, and M. Grazzini, Phys. Lett. B **564**, 65 (2003); Nucl. Phys. **B737**, 73 (2006); P. F. Monni, E. Re, and P. Torrielli, Phys. Rev. Lett. **116**, 242001 (2016).
[7] A related topic of jet-veto resummation in Higgs production is discussed in Refs. [8].
[8] I. W. Stewart, F. J. Tackmann, J. R. Walsh, and S. Zuberi, Phys. Rev. D **89**, 054001 (2014); T. Becher, M. Neubert, and L. Rothen, J. High Energy Phys. 10 (2013) 125; A. Banfi, P. F. Monni, G. P. Salam, and G. Zanderighi, Phys. Rev. Lett. **109**, 202001 (2012); F. J. Tackmann, J. R. Walsh, and S. Zuberi, Phys. Rev. D **86**, 053011 (2012); T. Becher and M. Neubert, J. High Energy Phys. 07 (2012) 108.
[9] R. K. Ellis, I. Hinchliffe, M. Soldate, and J. J. van der Bij, Nucl. Phys. **B297**, 221 (1988).
[10] B. Field, S. Dawson, and J. Smith, Phys. Rev. D **69**, 074013 (2004); W. Y. Keung and F. J. Petriello, Phys. Rev. D **80**, 013007 (2009); O. Brein, Phys. Rev. D **81**, 093006 (2010).
[11] A. Banfi, P. F. Monni, and G. Zanderighi, J. High Energy Phys. 01 (2014) 097.
[12] See Ref. [13] for recent attempts to understand the origin of these logarithms and the possibility to resum them.
[13] K. Melnikov and A. Penin, J. High Energy Phys. 05 (2016) 172; F. Caola, S. Forte, S. Marzani, C. Muselli, and G. Vita, J. High Energy Phys. 08 (2016) 150.
[14] M. Grazzini and H. Sargsyan, J. High Energy Phys. 09 (2013) 129.
[15] C. Anastasiou, C. Duhr, F. Dulat, E. Furlan, T. Gehrmann, F. Herzog, A. Lazopoulos, and B. Mistlberger, J. High Energy Phys. 05 (2016) 058.
[16] F. Bishara, U. Haisch, P. F. Monni, and E. Re, Phys. Rev. Lett. **118**, 121801 (2017).
[17] P. F. Monni, E. Re, and P. Torrielli, Phys. Rev. Lett. **116**, 242001 (2016).
[18] P. Bärnreuther, M. Czakon, and P. Fiedler, J. High Energy Phys. 02 (2014) 078; S. Borowka, N. Greiner, G. Heinrich, S. P. Jones, M. Kerner, J. Schlenk, and T. Zirke, J. High Energy Phys. 10 (2016) 107; 10 (2016) 107.
[19] L. Adams, C. Bogner, and S. Weinzierl, J. Math. Phys. (N.Y.) **56**, 072303 (2015); **57**, 032304 (2016); E. Remiddi and L. Tancredi, Nucl. Phys. **B907**, 400 (2016); L. Adams, C. Bogner, A. Schweitzer, and S. Weinzierl, J. Math. Phys. (N.Y.) **57**, 122302 (2016); R. Bonciani, V. Del Duca, H. Frellesvig, J. M. Henn, F. Moriello, and V. A. Smirnov, J. High Energy Phys. 12 (2016) 096; A. Primo and L. Tancredi, Nucl. Phys. **B916**, 94 (2017); A. von Manteuffel and L. Tancredi, J. High Energy Phys. 04 (2017) 083; H. Frellesvig and C. G. Papadopoulos, arXiv:1701.07356.
[20] K. Melnikov, L. Tancredi, and C. Wever, J. High Energy Phys. 11 (2016) 104.
[21] R. Mueller and D. G. Öztürk, J. High Energy Phys. 08 (2016) 055.
[22] K. Melnikov, L. Tancredi, and C. Wever, Phys. Rev. D **95**, 054012 (2017).
[23] C. R. Schmidt, Phys. Lett. B **413**, 391 (1997).
[24] V. Del Duca, W. Kilgore, C. Oleari, C. Schmidt, and D. Zeppenfeld, Phys. Rev. Lett. **87**, 122001 (2001); Nucl. Phys. **B616**, 367 (2001).
[25] T. Neumann and C. Williams, Phys. Rev. D **95**, 014004 (2017).
[26] F. Cascioli, P. Maierhöfer, and S. Pozzorini, Phys. Rev. Lett. **108**, 111601 (2012).
[27] The OPENLOOPS one-loop generator by F. Cascioli, J. Lindert, P. Maierhöfer, and S. Pozzorini is publicly available at http://openloops.hepforge.org.
[28] S. Kallweit, J. M. Lindert, P. Maierhöfer, S. Pozzorini, and M. Schönherr, J. High Energy Phys. 04 (2016) 021; S. Höche, P. Maierhöfer, N. Moretti, S. Pozzorini, and F. Siegert, Eur. Phys. J. C **77**, 145 (2017).
[29] T. Jezo, J. M. Lindert, P. Nason, C. Oleari, and S. Pozzorini, Eur. Phys. J. C **76**, 691 (2016).
[30] F. Cascioli, T. Gehrmann, M. Grazzini, S. Kallweit, P. Maierhöfer, A. von Manteuffel, S. Pozzorini, D. Rathlev, L. Tancredi, and E. Weihs, Phys. Lett. B **735**, 311 (2014);

D. de Florian, M. Grazzini, C. Hanga, S. Kallweit, J. M. Lindert, P. Maierhöfer, J. Mazzitelli, and D. Rathlev, J. High Energy Phys. 09 (2016) 151; M. Grazzini, S. Kallweit, S. Pozzorini, D. Rathlev, and M. Wiesemann, J. High Energy Phys. 08 (2016) 140.

[31] A. Denner, S. Dittmaier, and L. Hofer, Comput. Phys. Commun. **212**, 220 (2017); A. Denner and S. Dittmaier, Nucl. Phys. **B658**, 175 (2003); **B734**, 62 (2006); **B844**, 199 (2011).

[32] P. Nason, J. High Energy Phys. 11 (2004) 040; S. Frixione, P. Nason, and C. Oleari, J. High Energy Phys. 11 (2007) 070; S. Alioli, P. Nason, C. Oleari, and E. Re, J. High Energy Phys. 06 (2010) 043; T. Jezo and P. Nason, J. High Energy Phys. 12 (2015) 065.

[33] S. Frixione, Z. Kunszt, and A. Signer, Nucl. Phys. **B467**, 399 (1996).

[34] J. Alwall, Q. Li, and F. Maltoni, Phys. Rev. D **85**, 014031 (2012); E. Bagnaschi, G. Degrassi, P. Slavich, and A. Vicini, J. High Energy Phys. 02 (2012) 088; R. V. Harlander, H. Mantler, and M. Wiesemann, J. High Energy Phys. 11 (2014) 116; M. Buschmann, D. Goncalves, S. Kuttimalai, M. Schönherr, F. Krauss, and T. Plehn, J. High Energy Phys. 02 (2015) 038; K. Hamilton, P. Nason, and G. Zanderighi, J. High Energy Phys. 05 (2015) 140; E. Bagnaschi and A. Vicini, J. High Energy Phys. 01 (2016) 056; E. Bagnaschi, R. V. Harlander, H. Mantler, A. Vicini, and M. Wiesemann, J. High Energy Phys. 01 (2016) 090; R. Frederix, S. Frixione, E. Vryonidou, and M. Wiesemann, J. High Energy Phys. 08 (2016) 006; N. Greiner, S. Höche, G. Luisoni, M. Schönherr, and J. C. Winter, J. High Energy Phys. 01 (2017) 091.

[35] R. V. Harlander, T. Neumann, K. J. Ozeren, and M. Wiesemann, J. High Energy Phys. 08 (2012) 139.

[36] R. D. Ball *et al.* (NNPDF Collaboration), J. High Energy Phys. 04 (2015) 040.

[37] We calculated this value using the program RunDec [38], with the input value $m_b^{\overline{\rm MS}}(m_b^{\overline{\rm MS}}) = 4.2$ GeV.

[38] K. G. Chetyrkin, J. H. Kuhn, and M. Steinhauser, Comput. Phys. Commun. **133**, 43 (2000).